Study of Mechanical and Microstructural Properties of Titanium chips Fabricated by Large Strain Machining Process

A dissertation submitted in partial fulfilment of requirement for the award of degree of

Master of Engineering

in

Production Engineering

Submitted by

DEEPAK SHARMA

801585008

Under the guidance of

Dr. VINOD KUMAR SINGLA

Associate Professor

DEPARTMENT OF MECHANICAL ENGINEERING

THAPAR UNIVERSITY

PATIALA (PB), INDIA, 147004

July, 2017

Certificate

I hereby declare that the work done in this dissertation entitled "**Study of mechanical and microstructural properties of titanium chips fabricated by large strain machining process**" submitted towards partial fulfillment of requirement for award of degree of **Master of Engineering** in **Production Engineering, Thapar University, Patiala,** is an authentic record of the work carried out by me under the supervision and guidance of **Dr. Vinod Kumar Singla, Associate Professor, Mechanical Engineering Department, Thapar University, Patiala.**

The matter embodied in this report has not been submitted in part or full to any other university or institute for the award of any degree.

Dated: 17/07/2017

DEEPAK SHARMA
801585008

This is to certify that above declaration made by the student concerned is correct to the best of our knowledge and belief.

.....

Dr. Vinod Kumar Singla
Associate Professor
Mechanical Engineering Department
Thapar University, Patiala

Dedicated to

My loving parents…

Acknowledgements

I would like to express my deepest sense of gratitude and a very sincere thanks to my guide **Dr. Vinod Kumar Singla**, Associate Professor, Mechanical Engineering Department, Thapar University, Patiala for his sincere and invaluable guidance and full support which helped me in the accomplishment of this thesis report in present form. His dynamic and diligent enthusiasm has been highly instrumental in keeping my spirits high. His flawless and forthright suggestions blended with an innate intelligent application have crowned my task with success.

I am also thankful to **Dr. S. K. Mohapatra,** Head of Department, Mechanical Engineering, for providing us with the adequate infrastructure in carrying out the work. I would like to thank the entire faculty and staff of Mechanical Engineering Department and my friends who devoted their valuable time and help me in all possible ways towards successful completion of this work. I thanks all those who have contributed directly or indirectly to this work.

Lastly, I would like to thank my family for their years of guidance, support, and encouragement. It would not have been possible without them to reach upto this point. They have always wanted the best for me and I admire their determination and sacrifices.

Deepak Sharma

801585008

ABSTRACT

Titanium alloys have gained attention in the fields of aerospace and defense sectors due to their unique strength and lightweight. A unique severe plastic deformation method (SPD) of large strain machining (LSM) was used to fabricate chips of Ti6Al4V titanium alloy in the present investigation. Since the technique employed earlier don't match the current expectation and demand of the industry so, this technique solves the problem of previously employed technique to manufacture bulk nanostructured materials. In the present work experimental, investigation and property analysis is carried out. Response surface methodology (RSM) has been used to develop the input output relations. Feed, rake angle and speed have been considered as input parameters while shear strain, hardness and surface roughness have been considered as output parameters. Based on experiments carried out, Box-Behnken design technique has been used to develop nonlinear models. . Experiments are carried out in HMT LT21 lathe with the help of special design tool post The mechanical properties of the strips produced were measured by micro hardness tester. Also, the surface roughness and surface morphology of strips were studied using surface roughness tester and scanning electron microscope (SEM). While measuring the hardness of strips produced, it was revealed that hardness of strips was more as compared to the alloy. Similarly properties of surface were found to be improved.

Keywords: SPD, RSM, LSM, Nano structured materials

TABLE OF CONTENTS

LIST OF FIGURES

LIST OF TABLES

Nomenclature

λ	Chip thickness ratio
Υ	Shear strain
t_c	Deformed chip
t	Undeformed chip
E_{eff}	Effective strain

Greek symbol

°	Degree
µ	Micro

Abbreviations

LSM	Large strain machining
LSEM	Large strain extrusion machining
ECAP	Equal channel angular pressing
HPT	High pressure torsion
ARB	Accumulative roll bonding
SEM	Scanning electron microscope
XRD	X-ray diffraction
DF	Degree of freedom
ANNOVA	Analysis of variance

CHAPTER 1

INTRODUCTION

1.1 Nanostructured Materials:

From the past two decade the use of nanostructured materials in the field of aerospace, defense, aviation and manufacturing has increased. Titanium and other light weight alloys has been extensively used in these fields. Since these alloys possess high strength, that's why they has been widely used in these fields. Nanostructured material possess excellent mechanical, physical and chemical properties therefore their demand has gained attention in near past. So research and development needs to be carried out across globe for the development of nanostructured material [1].

The grain size of nanostructured material varies from 1-10 nm (nanometers), they are different from their coarse grain counterpart. Nanostructured material possess significant mechanical properties such as high strength, low ductility and higher superplasticity at lower temperature as compared to their coarse grain counterpart. These extraordinary properties of nanostructured materials is due to smaller grain size as compared to their coarse grain counterpart [1]. The figure 1.1 shows different grain size for different materials [2].

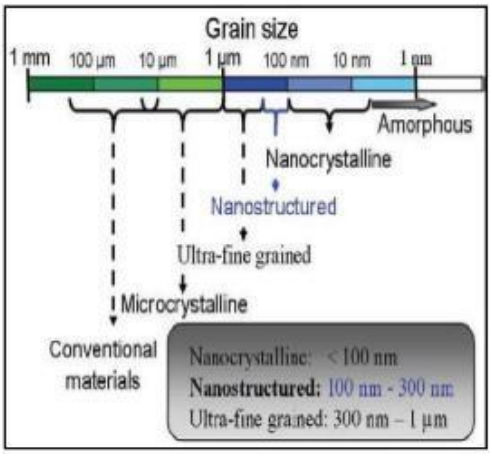

Figure 1.1: Grain size range for different materials [2]

1.2 Categories of nanostructured materials:

The first category of materials are those which have reduced dimension in form of nanometer sized particles. Inert gas condensation, various aerosol techniques are few methods to generate this class of material.

The second category of materials are those which has nanometer sized microstructure limited to thin surface region of the material. Laser beam and ion implantation are few technique to modify this class of nanostructured material.

The third category is actually a subgroup of second category in which the surface region is structured by a structural pattern on free surface. These type of nanostructured material can be synthesized by lithography.

Figure 1.2 shows classification based upon chemical composition and dimensionality of the crystallites [1].

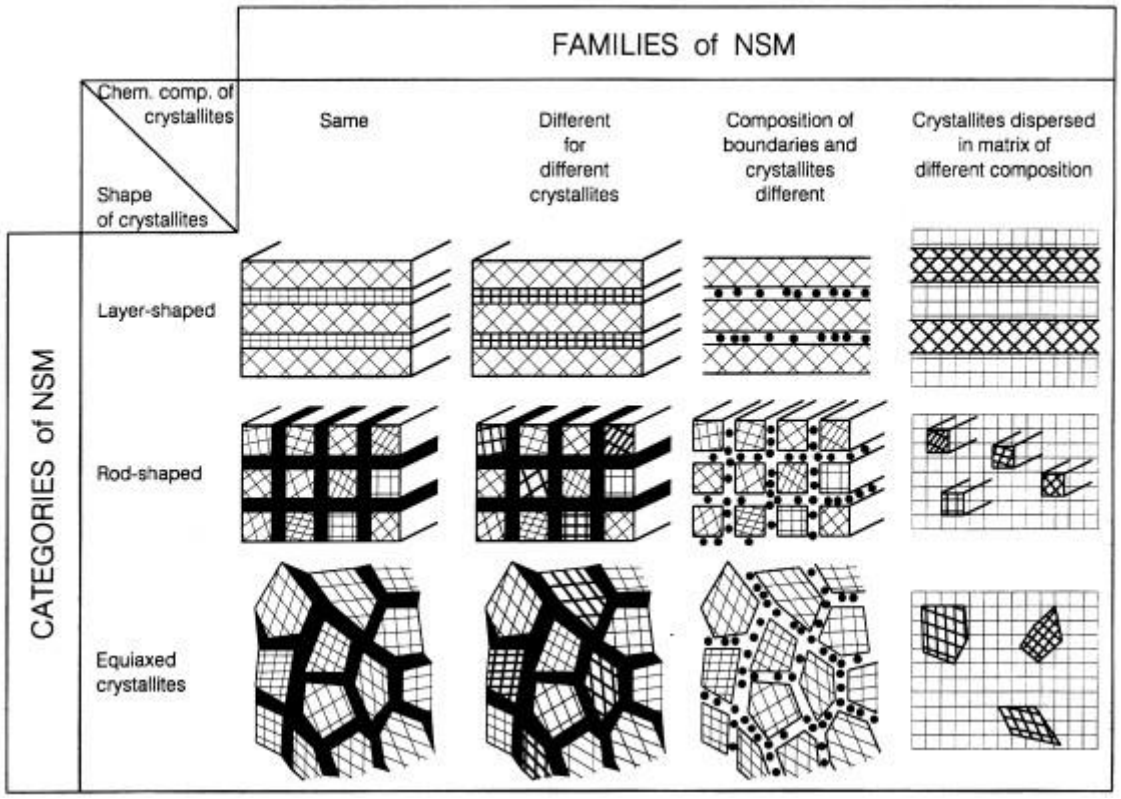

Figure 1.2: Classification of nanostructured material based upon chemical composition and dimensionality of the crystallites [1]

1.3 Properties of nanostructured materials:

Mechanical properties:

- High strength
- High hardness
- Low ductility
- High superplasticity

Physical and chemical properties:

- High thermal stability
- High wear resistance
- High corrosion resistance
- High electrical and magnetic properties [1]

1.4 Methods for creating nanostructured materials:

Mainly two categories of approach are used to synthesize nanostructured materials. The first one is bottom-up approach and the second approach is top-down approach.

Bottom-up approach: These approaches include the miniaturization of materials component (up to atomic level) with self-assembly process leading to the formation of nanostructures. Bottom-up method starts with atoms or molecules and build upto nanostructures. This method is less expensive in comparison to the other counterpart method [4].

Few process under bottom-up approach which will be discussed later are

- Inert gas condensation
- Electrodeposition
- High energy ball milling

Top-down approach: These approaches use larger (macroscopic) initial structures, which can be externally controlled in the processing of nanostructures. Top-down methods begin with pattern on larger scale which is reduced to a nanoscale. This method is not cheap and not quick to manufacture [4].

Few process under top-down approach which will be discussed later are

- Equal channel angular pressing (ECAP)
- High pressure torsion (HPT)
- Accumulative roll bonding (ARB)

Processes which has been stated above will be discussed in details below:

1.4.1 Inert gas condensation:

In inert gas condensation process a material (metal) is evaporated from a heated chamber, the vaporized material comes in contact with the inert gas (argon or helium) which is been backfilled into chamber at low pressure losses its energy by colliding with the inert gas. The metal vapor cools and becomes supersaturated to form nanoparticles. These nanoparticles are of the size of 1-100 nm (nanometer) which is collected and may be compacted to produce a dense nanomaterial [4]. The figure 1.3 shows the schematic diagram of inert gas condensation.

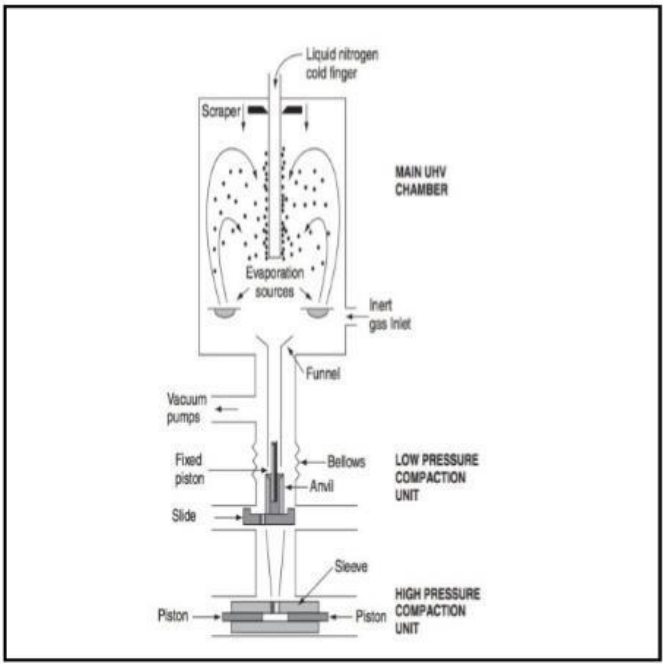

Figure 1.3: Schematic diagram of inert gas condensation [4]

1.4.2 Electrodeposition:

The electrodeposition is a well-established method to deposit metal layer on a conducting substrate.

Ion in solution are deposited onto the negatively charged cathode. The process is relatively cheap and fast and allows complex shape to manufacture at low temperatures also. The thickness of layer deposited depends on the current density and the time for which the current flows. This method can deposit nanostructured material including metal oxides [2].

The figure 1.4 shows the schematic diagram of electrodeposition.

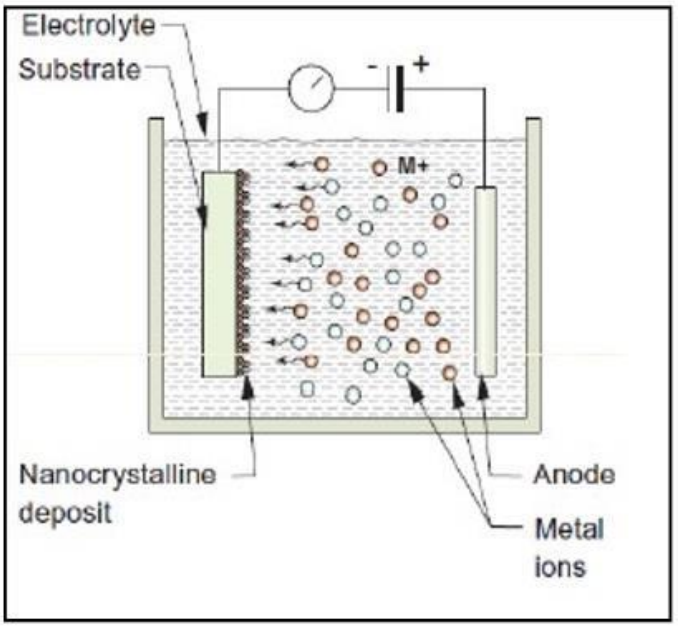

Figure 1.4: Schematic diagram of electrodeposition [2]

1.4.3 High energy ball milling:

This is the simplest method of making nanoparticle in the form of powder. It consist of container filled with tungsten carbide or hardened steel balls. Material is fed as flakes. Ratio of balls to material flakes should be 2:1. High energy ball milling consist of one turn disc and four bowls. Both turn disc and bowls rotate in opposite direction this creates a centrifugal force which is applied on the material and milling balls. The material is fractured and cold welded under this impact [6].

The figure 1.5 shows the schematic diagram of high energy ball milling.

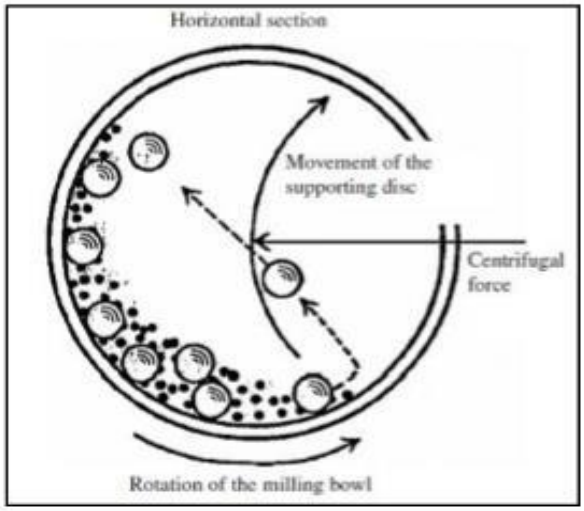

Figure 1.5: Schematic diagram of high energy ball milling [6]

1.4.4 Equal channel angular pressing:

V. Segal et al. in 1981 introduced this method to produce nanostructure material by a simple shear. It was applied to produce ultra fine grain in metals as shown in fig 1.6 and 1.7 respectively. In ECAP a channel is formed into a die which is at an abrupt angle of 90˚. The sample to be machined is fit into the channel and pressed using a plunger.

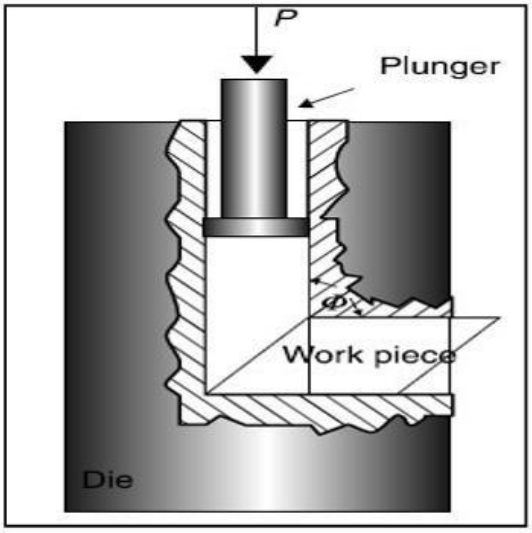

Figure 1.6: Schematic diagram of Equal channel angular pressing [3]

ECAP is uniquely different from other conventional industrial processes such as drawing, extrusion or rolling because the crossection of the sample before and after pressing remains same in comparison to conventional process where there is significant reduction in the crossection of the sample before and after pressing [2]. The figure 1.6 and 1.7 shows the schematic diagram of ECAP.

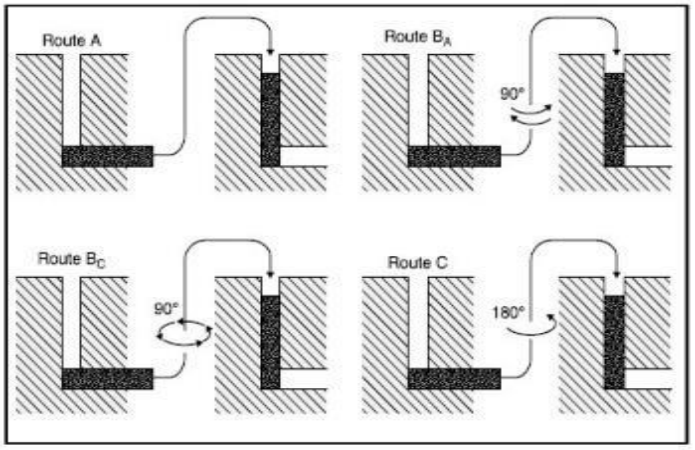

Figure 1.7: Schematic diagram of process of Equal channel angular pressing [3]

1.4.5 High pressure torsion (HPT):

High pressure torsion can be understood with the help of the figure 1.8. The sample which are processed under HPT are disc shaped. The sample is placed between anvils and when pressure P is applied in GPa it undergoes strained in torsion. When lower anvil turns shear straining of the sample occur due to friction forces. To produce a homogeneous nanostructure several turns is necessary to deform which will lead to a grain size of 100 nm or less.

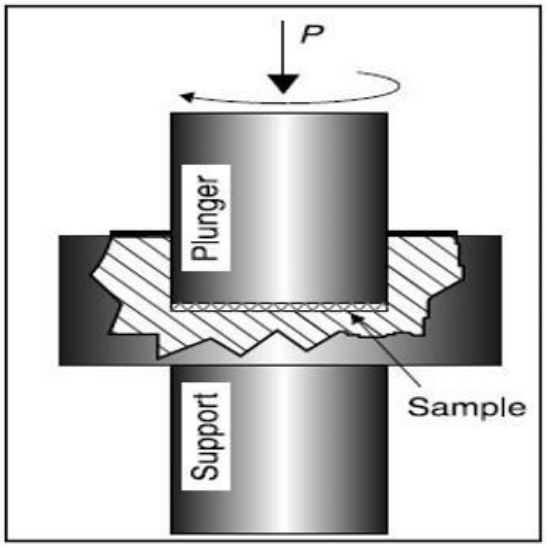

Figure 1.8: Schematic diagram of High pressure torsion [2]

1.4.6 Accumulative roll bonding (ARB):

Saito et al. in 1998 developed the concept of accumulative roll bonding. It is been depicted in figure 1.9.

ARB basically works on the principle of rolling deformation. Two sheets of same material is rolled between rollers after it is heated below recrystallization temperature thus, bonding the sheets together. Then this sheet is cut into two equal halves then they are stacked and the process is repeated several times.

ARB does not require specialized equipment other than rolling mill. The surface of the material to be joined must be clean for good bonding.

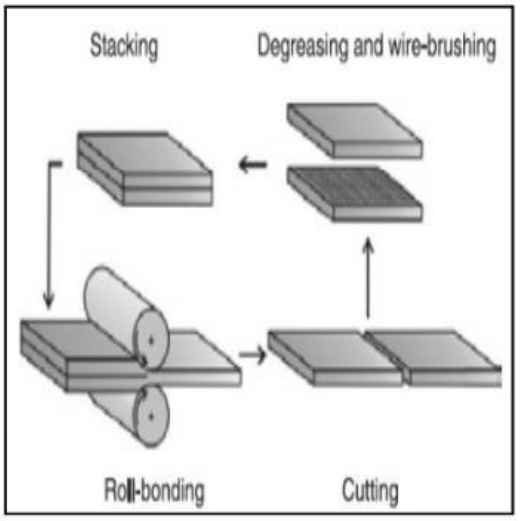

Figure 1.9: Schematic diagram of Accumulative roll bonding [2]

1.5 Limitation of Bottom up and Top down approach:

1. In order to create large plastic strain multiple stages of deformation are required.
2. It is found to be difficult to deform metals and alloys of high strength due to different constraints applied by operating tools.
3. Preheating is mandatory at elevated temperatures in few cases.
4. Not all materials can be prepared by these method.
5. The tools and equipment are very costly.
6. Oxides are produced in some cases which makes it difficult to processed material further.
7. Most of the processes are time consuming.

1.6 Introduction to Large strain machining:

In the past decade machining based deformation process has been emerged as a feasible alternative to conventional severe plastic deformation methods.

By imposing large uniform plastic strain in a single pass of a cutting tool, the chip formation due to it offers an alternative to produce nanostructured and UFG materials. Shear strain can vary from a range of 1-15 in various materials. But unlikely conventional methods, control over shape and dimension of fine grained chips is limited. But microstructure refinement can be done using large strain machining.

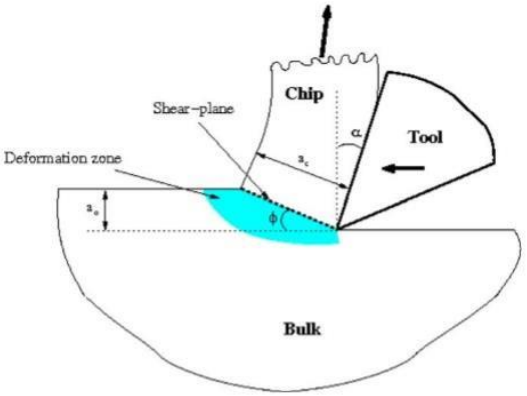

Figure 1.10: Mechanics of formation of chips [7]

CHAPTER 2
LITERATURE REVIEW

In this chapter we will be studying different research paper on LSM to get to know more about the process and different process parameters in order to decide the process parameters of present thesis work.

2.1 Literature Review:

Shankar et al. [7] used large stain machining to analyze the critical plastic deformation of titanium at near atmospheric temperature. It was found that nanocrystalline structure whose grain sizes around 100 nm have highest level of strain. Particle image velocimetry technique have been used to found out the parameters of the large-strain deformation field like strain rate and strain. It was concluded that microstructure was likely to the mirror and the values obtained of strain was smaller and important twinning was observed.

Shankar et al. [8] analyzed the properties of 6061 aluminium alloy. It was found that if peak-aged temper and over-aged temper were used for producing the chips; soften following heat treatment while those chips produced from the solution-treated state, these chips firstly gain strength then softening. It was also found that in case of single pass deformation, large strains apply.

Kim et al. [9] studied for enhancing the strength of 6061 aluminium alloy. It was found that with the addition of Pre- ECAP solid solution treatment in post- ECAP aging treatment, strength of 6061 aluminium alloy enhance as compare to pre-ECAP peak-aging treatment. It was also found that with the use of post-ECAP aged materials UTS and yield strength increases approximately 40% as compare to T6 treated commercial 6061 aluminium alloy.

Shekhar et al. [10] used Rate-Strain-Microstructure Mappings to determine the effect of Severe Plastic Deformation in Machining Elucidated. It was used rate-strain-microstructure (RSM) framework for determined the deformation parameters to the resulting deformed grain size and interface characteristics. It was concluded that RSM map determined delineates region where recrystallization will occur and hence conditions to produce coarse grained, low strength microstructure albeit thermally stable, and hence can be employed for high temperature applications.

Shekhar et al. [11] studied on Interactive Effects of Strain, Strain-Rate and Temperatures on Microstructure Evolution in High Rate Severe Plastic Deformation. By controlling the grain growth microstructure affected by temperature. It also affected the strain and strain rate parameters. These deformation factors can be used as fingerprint for the resultant microstructure. It was found that by continuous dynamic recrystallization operative under HRSPD conditions, where strain, strain rate and temperatures offer varying degrees of multimodality in the grain-size distributions.

Huang et al. [12] studied on severe plastic deformation of titanium. Infrared thermography technique was used to measure the Temperature rise in severe plastic deformation of titanium at small strain-rates. It was found that during the deformation temperature rise is small and unlike affected the material behavior. It was also found the temperature distribution in deformation zone is similar to the strain rate distribution zone.

Swaminathan et al. [13] used transmission electron microscopy (TEM) and orientation imaging microscopy (OIM) to analyze the microstructure of cooper chips produced by plain strain machining at atmospheric temperature. It was found that by changing the tool rake angle strain imposed on chips was varied.

Calistes et al. [14] used large-strain machining for controlling gradation of surface strains and nanostructuring. It was investigate that an upper bound model for the deformation, control of severe plastic deformation parameters on the machined surface is seen to be feasible, suggesting interesting opportunities for nano and micro scale engineering of surface microstructures by machining.

Kustas et al. [15] studied the level of porosity and other mechanical properties of strips fabricated from Aluminium 5052, they fabricated these strips through large strain machining process in which there is control over deformation of chips. There was reduction in the level of porosity because of continuous shear strain. Mechanical properties was also found within the range as processed by conventionally rolled and annealed strips.

Deng et al. [16] have studied the thermal stability of nanostructured fabricated by LSEM of Al alloy. Annealing treatment for different time frame at different temperature were done. These structure found to be hard under 200˚C but at 300˚C and above hardness decreases. When annealing time was increased at 200˚C recrystallization occur.

Sagapuram et al. [17] have demonstrated to produce sheets through LSEM for Mg and Ti alloys. They investigated effects of different process parameters on microstructure and sheet

flow. They found as the sheet thickness increases the fracture was noticeable as compared to other ductile metal and alloys such as Cu and Al. Also they found improved formability and recrystallized microstructure.

Brown et al. [18] have controlled the deformation field by controlling the deformation parameters such as strain (1-15), temperature (.4 T_m) and strain rate (10-100000 s^{-1}) for Copper. It was found that bi modal microstructure was formed which were micron sized and lead to recrystallization in deformation zone.

Chandrasekhar et al. [19] have highlighted the capability to produce nanostructured grain size which have controlled microstructure for magnesium alloy. Controllable parameters such as chip thickness ratio and rake angle were responsible for fabrication of predetermined texture of magnesium alloy.

Shankar et al. [20] have studied the characteristic of aluminium alloy (6061-T6) chips fabricated by 2-D machining. By changing the tool geometry and implement different strain, chips were fabricated and studied. The result were compared to that fabricated by ECAP and it was found that the micro-hardness values were greater than counterpart ECAP fabricated structure.

Swaminathan et al. [21] have analyzed deformation fields in large strain machining for dirrent metal and alloys. The result states that with the help of large strain machining the manufacturing of nanostructured material along with the experimental configuration to study the large strain deformation phenomena can be achieved. The effect of strains, temperature on microstructure was carried out during the experimental results.

Mann et al. [22] have demonstrated the use of modulation assisted machining. Discrete chips were fabricated using MAM arrangement. Al 6061-T6 material was used to fabricate chips of discrete nature. Discrete chips may be of powder form depending on the modulation. Large strain deformation enhance the hardness and strength of the microstructure.

Kustas et al. [23] employed LSEM to study its practicability in eliminating porosity from a casted ingot of aluminum 5052 acquired from hydrogen entrapment during melting & casting and volumetric shrinkage during solidification. Optical microscopy of bulk and fabricated strips was performed to compare porosity level, which was followed by Limiting Dome Height (LDH) test to compare the mechanical properties of strips produced from LSEM and conventional rolling. Optical micrographs, of the strip indicated significant porosity reduction, due to high shear strain and hydrostatic pressure during extrusion. Mechanical behavior of LSEM strips from LDH test was discovered to be ranging within conventionally rolled and annealed strips.

Mert et al. [24] analyzed the mechanics of LSEM in which high deformation rate and high hydrostatic pressure have been applied in a single step on Magnesium alloy (MgAZ31B) for the continuous production of Mg alloys in bulk form to sheets and foil. Hydrostatic pressure and temperature in the deformation zone were found to be function of chip thickness ratio, rake angle. Capabilities to realize combinations of large strain, large hydrostatic pressure and low temperature levels, especially in a highly confined region (primary deformation zone), promoted the workability and grain refinement of alloys.

Lee et al. [25] have discussed about measuring of strain field in primary deformation zone. They have also analyzed tool chill interface in 2D machining. The velocity distributions in the primary deformation zone and along the tool rake face have been obtained by applying a particle image velocimetry (PIV) technique sequences of high-speed images of the chip-tool interface taken through the transparent tool.

Iglesias et al. [26] have analyzed the effect of wear resistance of nanostructured material of copper (Cu) fabricated by LSEM as a function of microstructure and sliding direction of ball on flat configuration under variable shear strain. The lowest wear volume was obtained when the sliding takes place in the perpendicular direction to that of grain orientation. The highest wear resistance was observed for nanostructured copper material with an elongated grain structure in the extrusion direction. The wear resistance of this anisotropic material depends on the sliding direction.

Iglesias et al. [27] discussed new machining-based manufacturing processes with the use of which, nanostructured materials could be manufactured much economically as compared to existing methods to do so. Shift from LSM to LSEM has been justified on PH13-8Mo Stainless steel since LSEM is combination of refinement of microstructure via large strain machining while shape and dimension of chips are controlled by extrusion, whereas in the former method only grain refinement was possible. Further a cost analysis was made considering machining cost/hour C, cutting velocity V, exit sheet (chip) thickness of t_c, chip thickness ratio and sheet width of w.

$$Cvol = \frac{\lambda . C}{3.6 t_c w V}$$

2.2 Conclusion drawn from literature review:

1. The effect of different parameters of tool geometry on LSM has been analyzed.

2. Formation of nanostructured strips with the help of large strain were discussed.

3. The most significant effect on the shear strain of the chips is because of rake angle and chip compression ratio.

4. Lower the rake angle higher will be the strain rate.

5. Smaller rake angle results in small microstructure compare to higher rake angle microstructure.

6. As chip thickness ratio decreases it will result in increase in effective strain and hence smaller grain size can be obtained.

7. The hardness of nanostructured chips was higher than bulk materials.

8. As shear strain was increased nanostructure refinement of UFG was found.

9. When both nanostructured material and microstructure material was compared in wear rate it was found that wear rate is more in microstructure materials.

10. Better formability was achieved when material was fabricated as sheet metal machining.

11. During study of thermal stability the hardness of UFG was increased upto certain temperature and further decreased on increasing the temperature.

12. By controlling parameters such as strain, temperature and strain rate bi modal microstructure was formed.

2.3 Research gaps from literature review:

1. A lot can be done to reduce temperature effects due to high speed at the cutting edge as different metals and their alloys possess different behavior under same temperature range.

2. The mechanics behind the deformation of metals and their alloys is yet to be explored using LSM.

3. Material which are difficult to machine such as Ti and its alloys needs to be machined using LSM.

4. Nanostructured chips fabricated using LSM needs to be study for corrosion.

5. Thicker chips with smaller grain sizes needs to be manufactured using LSM which will ease the manufacturing of bulk nanostructure material.

6. A lot of work can be done to study the thermal stability of nanostructured strips fabricated using LSM.

Based on the study of literature review on large strain machining the objective of present thesis work is obtained which will be discussed in next section.

CHAPTER 3

OBJECTIVE AND METHODOLOGY

Based on the study of literature review on large strain machining the objective of present thesis work is obtained which will be discussed in next section.

3.1 Objective of present work:

1. Fabrication of nanostructure chips of titanium alloy using LSM under different process parameters.
2. Detailed roughness and micro hardness analysis of different chips produced by LSM.
3. To study the deformation level changes of the chips produced by LSM.
4. Study of strain by varying the machining parameters.

3.2 Material selection:

Since a lot of work has been done on material which are easy to machined, so material which is hard to fabricate was taken into consideration in present thesis work.

Titanium alloy (Ti6Al4V) which is hard to machined was taken as material for present thesis work. Ti6Al4V is used in the present thesis work because of following reasons.

1. This alloy has high tensile strength and toughness.
2. They are light in weight.
3. They have extraordinary corrosion resistance properties.
4. This grade of titanium alloy withstand under extreme temperature limits.
5. Wide application in the field of defense, aviation, spacecraft and biomedical.

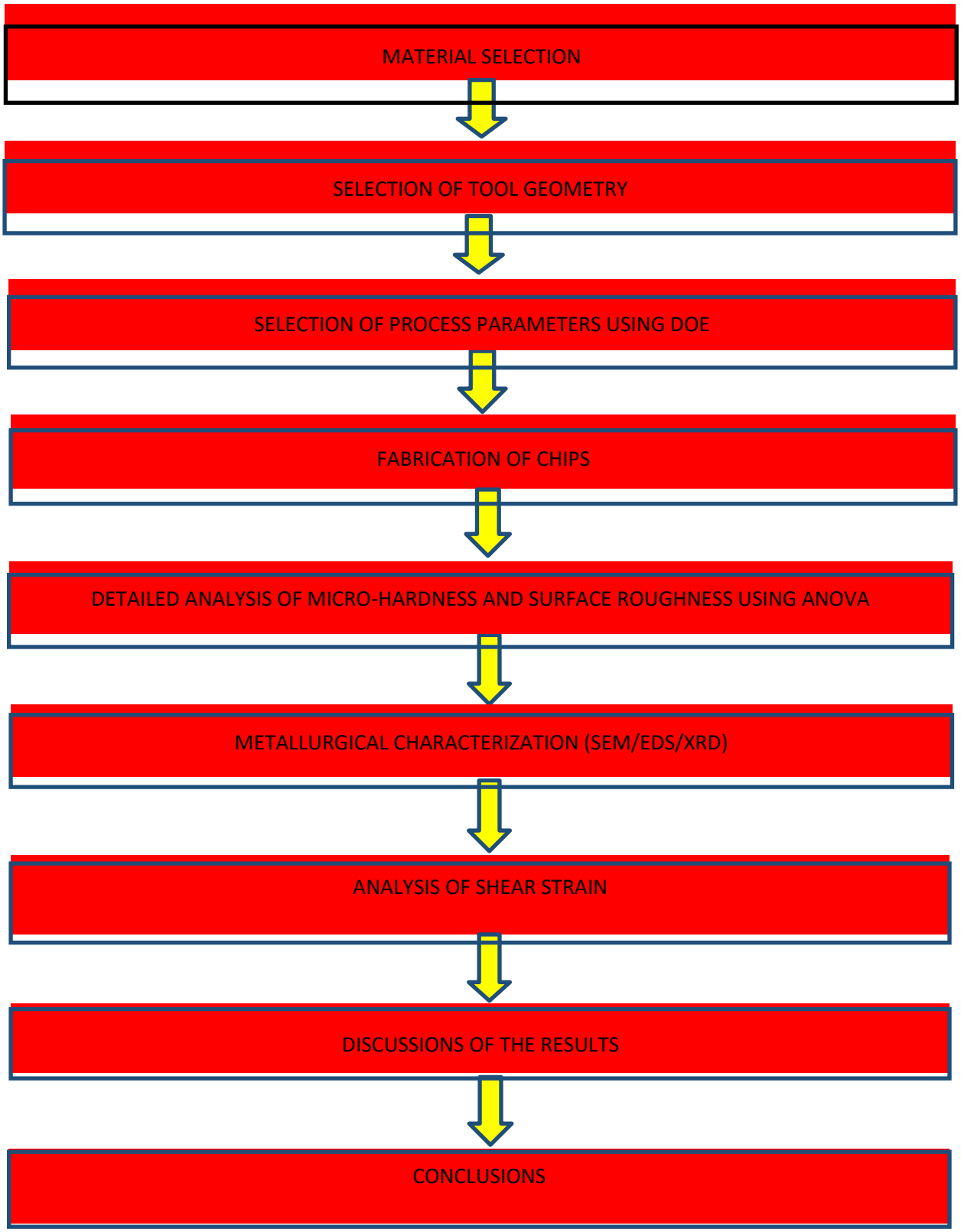

Figure 3.1: Flow chart of work plan

Table 3.1: Composition of Ti6Al4V

Alloy	Ti	Al	V	Fe	O	C	N	H
Ti6Al4V	87.6-91%	5.5-6.75%	3.5-4.5%	≤0.4%	≤0.02%	≤0.08%	≤0.05%	≤.015%

Table 3.2: Properties of Ti6Al4V

S. No	PARAMETER	VALUE
1.	DENSITY	4.429-4.512 Mg/m^3
2.	DUCTILITY	.05-.18
3.	HARDNESS	3370-3730 Mpa
4.	MELTING TEMPERATURE	1178-1933 K

3.3 Experimental setup:

In the current investigation, effect of various large strain machining process parameters are studied. The process parameters are tool rake angle, feed and speed. Titanium alloy is used as a raw material. 2HP universal lathe with rotary configuration is used to produce the strips. Special design tools made of carbide tip were used to replace conventional cutting tool. Special designed tool post was also prepared. The machining is done radially at different speeds and feed. Machining was done without using lubricant. With continuous feeding of tool, strips of different lengths were fabricated from the tool. Experiments were conducted as per Box-Behnken Design (BBD) with the help of design of expert (DOE). The entire experiments were carried out in Machine tool Lab, Thapar University Patiala.

(a)

(b)

(c)

Figure 3.2: (a) +5˚ Rake angle tool (b) 0˚ Rake angle tool (c) -5˚ Rake angle tool

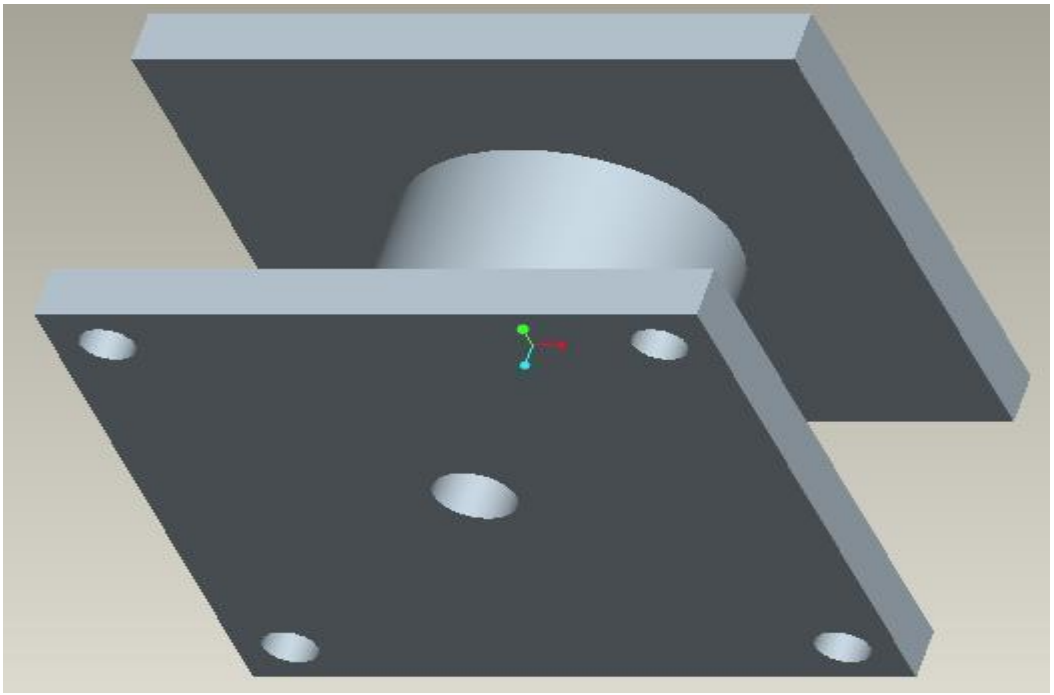

Figure 3.3: Designed and fabricated tool post

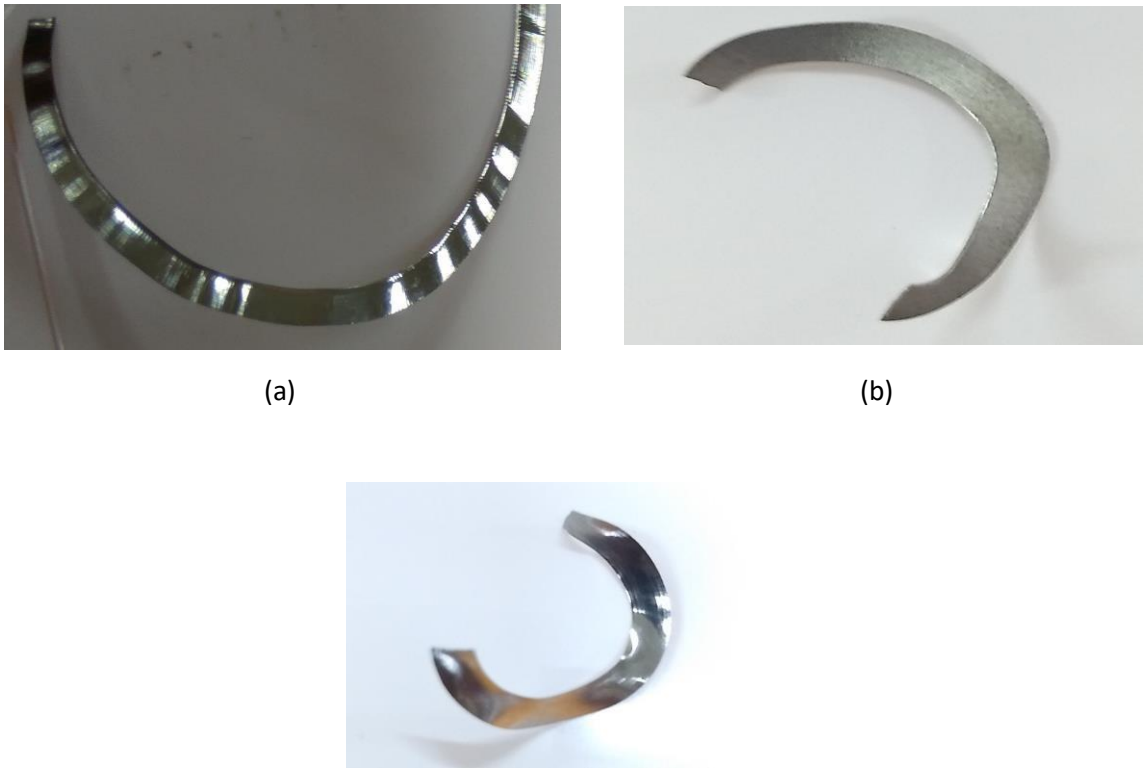

(a) (b)

(c)

Figure 3.4: (a) Chips at 720 rpm (b) Chips at 570 rpm (c) Chips at 420 rpm

3.4 Equipment used:

Micro Hardness and Surface Roughness test were performed on all the strips. For surface morphology Scanning Electron Microscope (SEM) was used. To study crystalline grains size XRD machine was used. The equipment's used for measurement of these responses are given below

3.4.1 Micro hardness tester:

Micro hardness analysis was done to measure the penetration resistance of the specimen. Measurements were done on a computer Interfaced Micro Hardness Tester (Model: MVH2), available at Thapar University, Patiala. The micro hardness measurement is dependent on the diameter of indentation produced on the samples. Indentation was done with a diamond cone indenter at a constant load of 100gm/mm^2 for a dwell period of 20 sec with Quantimet software. 40 MP cameras were used for observing / focusing images.

Figure 3.5: Micro hardness testing machine Model: MVH2 (Courtesy: Advance Measurement Lab, Thapar university, Patiala)

3.4.2 Surface roughness tester:

Surface roughness was measured using the Mitutoyo model SJ-400, Germany. The equipment uses the stylus method of measurement, has profile resolution of 12 nm and measures roughness up to 100 µm. A tracing length of 4.8 mm was used for analysis. Surface Roughness values were taken two times for each trial and average was used for analysis.

Figure3.6: Surface roughness tester SJ-400 (Courtesy: Metrology lab Thapar university, Patiala)

3.4.3 X-ray diffraction:

XRD analysis was performed using panalytical X-Pert Pro diffractometer (θ - 2θ) equipped with Cu-Kα radiation (λ = 1.5418 Å). The specimens for X-ray diffraction examination were prepared by grinding with SiC papers of up to 2000 grit size to flat grounded surfaces for performing 2-theta scanning of all samples for quantitative analysis of deformation behavior at different process conditions.

Figure 3.7: X-RAY Diffraction (Courtesy: SAI Lab, Thapar University, Patiala)

3.4.4 Scanning electron microscope:

In SEM high energy electron focus beam used for generate different variety signals to get information about sample morphology, chemical composition, and crystalline structure.

The SEM used for this study is a highly accurate and precise instrument (Make: JSM-6510LV, JEOL Ltd, Tokyo, Japan) for fast characterization and imaging of fine structures and has a magnification range from 5–300,000 X (printed as a 128 mm x 96 mm micrograph). It was used to study the worn surfaces and investigate the wear mechanism. This facility is available at SAI Labs, Thapar Technology Campus, Patiala.

Figure 3.8: Scanning electron microscope (Courtesy: SAI Lab, Thapar University, Patiala)

CHAPTER 4

DESIGN OF EXPERIMENTS

4.1 Introduction:

In this chapter we will be developing the design for surface roughness and micro hardness of Ti6Al4V chips fabricated from large strain machining. The impact of various input parameters on responses have been studied after producing chips. The various input parameters were rake angle, feed and speed. Experiments were designed by using Design expert software. This software runs the experiments randomly. Box-behnken design technique was used for conducting the experiment. It plays an important role for achieving the high efficiency of the response surface methodology. Box Behnken design experiments require lesser experiments as compare to Central Composite design. The proposed Box Behnken design requires 17 experiments since there are three parameters.

4.2 Factors selection:

The process parameters with their different levels have been selected after exhaustive literature survey. The selected parameters are shown in Table 4.1.

Table 4.1: Selected Factors and their ranges

FACTORS	LEVEL 1	LEVEL 2	LEVEL 3
Tool Rake Angle (^{O})	-5	0	5
SPEED(m/min)	40	80	120
FEED (mm)	0.05	0.10	0.15

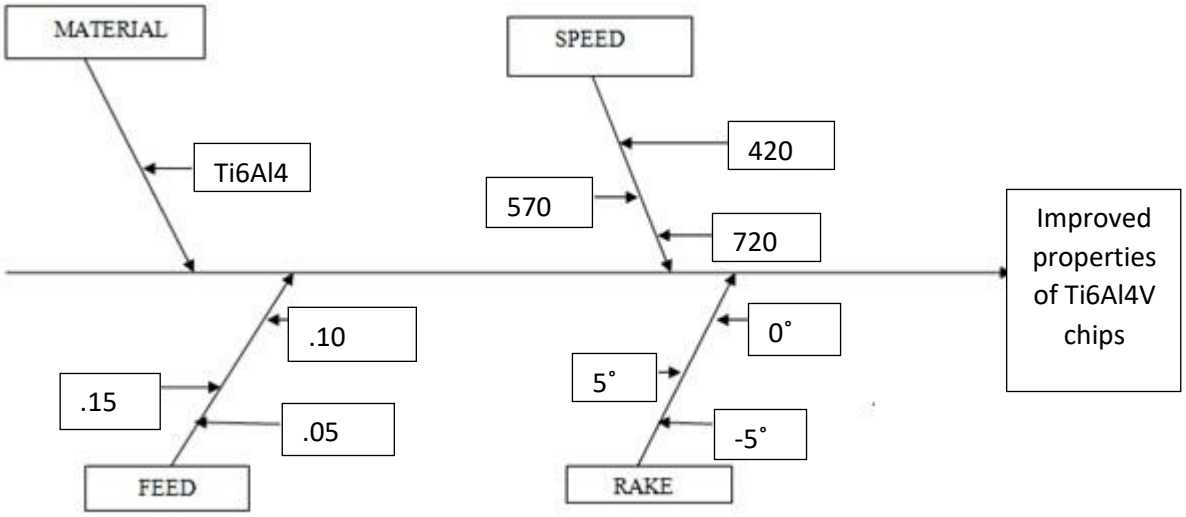

Figure 4.1: Cause and effect diagram

4.3 Box-Behnken Design:

Response surface methodology (RSM) is used for achieving the high efficiency of the response surface methodology. Response surface methodology (RSM) is a statistical technique which is used to maximize the output parameters. This technique is used in developing new technical studies. This technique is very cost effective.

The efficiency of Box-Behnken design is higher for an experiment involving three factors and three levels. The proposed Box Behnken design have 17 experiments. The experiments in software run randomly. Design expert software used for determining 2D and 3D plots. These graphs gives clear idea of the effect of process variable over other variable. Further the model was verified by performing experiments, taking two sets of random input values. The response values obtained through experiments are similar with the equation values using the model.

The experimental data for BBD is as follows

Table 4.2: Trail condition using BBD

STD	RUN	A:Rake(^{o})	B:Speed(rpm)	C:Feed(mm)
10	1	0	720	0.05
12	2	0	720	0.15
6	3	5	570	0.05

4	4	5	720	0.10
1	5	-5	420	0.10
3	6	-5	720	0.10
8	7	5	570	0.15
14	8	0	570	0.10
5	9	-5	570	0.05
15	10	0	420	0.10
11	11	0	420	0.15
17	12	0	570	0.10
13	13	0	570	0.10
7	14	-5	570	0.15
16	15	0	570	0.10
9	16	0	420	0.05
2	17	5	420	0.10

4.4 Analysis of results:

The experimental data collected as per BBD was used.

The result of Micro Hardness and Surface Roughness for Ti6Al4V is shown in Table 3.5

Table 4.3: Experimental obtained values of Micro hardness and surface roughness of Ti6Al4V chips

STD	RUN	A:Rake(^{o})	B:Speed (rpm)	C:Feed(mm)	RESPONSE: Micro hardness (HV)	Response: Surface Roughness(µm)
10	1	0	720	0.05	374.49	0.36
12	2	0	720	0.15	374.93	0.32
6	3	5	570	0.05	393.13	0.48
4	4	5	720	0.10	372.14	0.38
1	5	-5	420	0.10	416.62	0.42
3	6	-5	720	0.10	377.66	0.46

8	7	5	570	0.15	394.87	0.56
14	8	0	570	0.10	397.98	0.39
5	9	-5	570	0.05	402.09	0.63
15	10	0	570	0.10	413.68	0.38
11	11	0	420	0.15	414.96	0.31
17	12	0	570	0.10	398.24	0.37
13	13	0	570	0.10	398.99	0.40
7	14	-5	570	0.15	401.88	0.54
16	15	0	570	0.10	400.37	0.41
9	16	0	420	0.05	413.12	0.44
2	17	5	420	0.10	410.71	0.37

Further detailed analysis of responses will be discussed in chapter to be followed.

CHAPTER 5

RESULTS AND DISCUSSION

5.1 Introduction:

The effect of various process parameters such as (rake angle, feed and speed) on mechanical properties such as micro hardness, surface roughness. Effect of shear strain and surface morphology was also analyzed. Ti6Al4V titanium alloy cylindrical rod of 60mm dia was used for this experimental work. Design Expert software was used for experimental work. In this proposed investigation all the three factors were varied at three levels. After conducting the 17 trials the mean value of all the factors are tabulated.

5.2 Result and analysis of Ti6Al4V chips:

The experimental data collected as per BBD was used. Following result and analysis was obtained.

5.2.1 Analysis for micro hardness:

Micro Hardness of strips was measured by Vicker hardness tester machine.

The equation developed for response hardness is given below:

$$\text{MICROHARDNESS}=398.84-3.42\times A-19.44\times B+0.44\times C-0.49\times A\times A-4.17\times B\times B-0.35\times C\times C+0.04.\times A\times B+0.43\times A\times C-0.35\times B\times C$$

Table 5.1: ANOVA table for micro hardness

SOURCE	SUM OF SQUARES	DF	MEAN SQUARE	F-VALUE	PROB>F	% contribution	STATUS
Model	3488.60	9	387.62	387.85	<0.0001		Significant
A	93.43	1	93.43	93.49	<0.0001	2.66	Significant
B	3326.42	1	3326.42	3328.36	<0.0001	95.02	Significant
C	1.56	1	1.56	1.56	0.2520	0.044	Not Significant
A^2	0.99	1	0.99	0.99	0.3528	0.02	Significant
B^2	72.92	1	72.92	72.96	<0.0001	2.08	Significant
C^2	0.51	1	0.51	0.51	0.4985	0.014	Not Significant

AB	.00722	1	0.00722	0.007	0.9346	0.0002	Not Significant
AC	0.73	1	0.73	0.73	0.4207	0.020	Not Significant
BC	0.49	1	0.49	0.49	0.5064	0.013	Not Significant
Residual	7.00	7	1.00				Not Significant
Lack of fit	3.55	3	0.89	0.77	0.2043		Not Significant
Pure Error	3.45	4	1.15			.098	
Cor total	3495.59	16					

Significant Factor*:* A, B, B^2

Insignificant factor*:* A^2 , C, C^2, AC, BC, AB

Following things can be observed from analysis:

1. Model "F-Value" is 387.85 which imply model is significant. There is only 0.01% chance that model with this large value could occur due to noise.

2. Values of "Prob>F" lest than 0.05 indicates that model terms are significant. For given model A (Rake angle), B (Speed), B^2 (square of speed) are significant.

3. Values greater than 0.05 are totally insignificant.

4. The "Lack of Fit-F value" of 0.77 implies that Lack of Fit is not significant relative to pure error.

5. As we can see B contributed maximum to the model with % contribution 95.02 %. So it is the most significant factor in the model.

There is 60.98% chance that "Lack of Fit-F value" this large could not occur due to noise.

Non significant lack of fit is good –We want model to be fit.

The values of R-Squared given by software are as follows

Table 5.2: Different ANOVA parameters

R-Squared	0.9980
Adj R-Squared	0.9954
Pred R-Squared	0.9847
Adeq Precision	59.628

- The "Pred R-Squared value" of 0.9847 is reasonable agreement with the "Adj R-Squared value" of 0.9954.

- "Adequate Precision" value measure signal of noise ratio. It is desirable to have ratio greater than 4. Ratio of 59.628 indicates adequate signal. Hence model can be used.

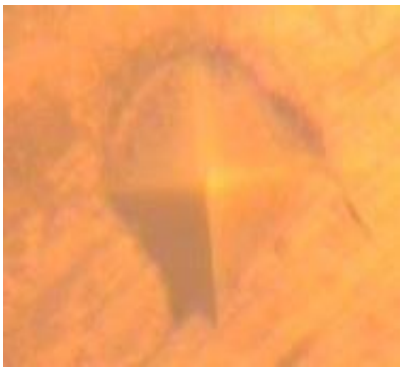

(a)Indentation at 0º, 420 rpm and .05 mm feed

(b) Indentation at 0º, 570 rpm and .05 mm feed

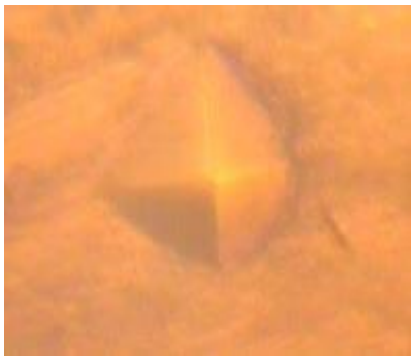

(c) Indentation at 5˚, 720 rpm and .05 feed

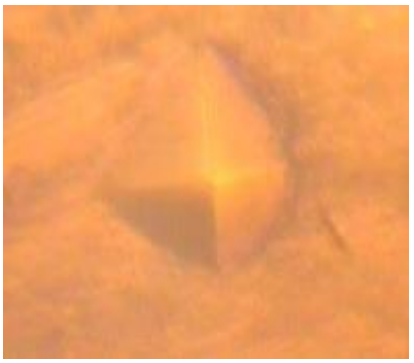

(d) Indentation at 5˚, 420 rpm and .05 mm feed

(e) Indentation at -5˚, 570 rpm and 0.5 mm feed

(f) Indentation at -5˚, 720 rpm and .05 mm feed

Figure 5.1: Indentation at chips for different trails

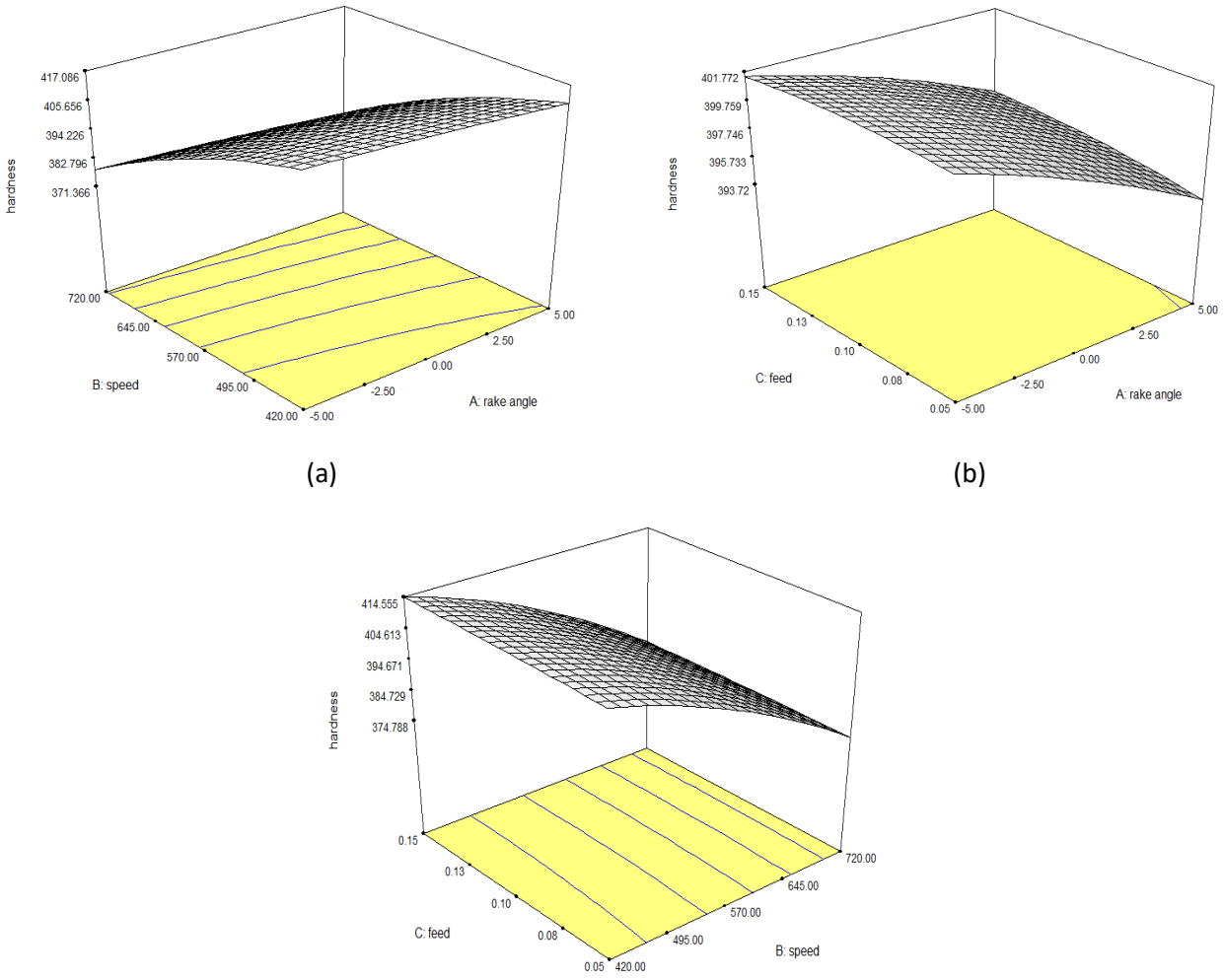

Figure 5.2: 3-D plot of variation of (a) speed and rake v/s micro hardness (b) feed and rake v/s micro hardness (c) feed and speed vs micro hardness

The effect of rake angle and speed is shown on hardness at different process parameter is shown in figure 5.3(a) and 5.3(b) respectively. The trend portrays reduction in hardness with increase in cutting speed (from 79 m/min to 136 m/min) and decrease in rake angle (from +5° to -5°). With decrease in rake angle, forces and stresses in the PDZ increases, causing a driving force to the dislocations piled up along the grain boundaries causes low angle grain boundaries, resulting in sub grain formation or grain refinement. This grain refinement increases the dislocation density causing increased hardness of the material

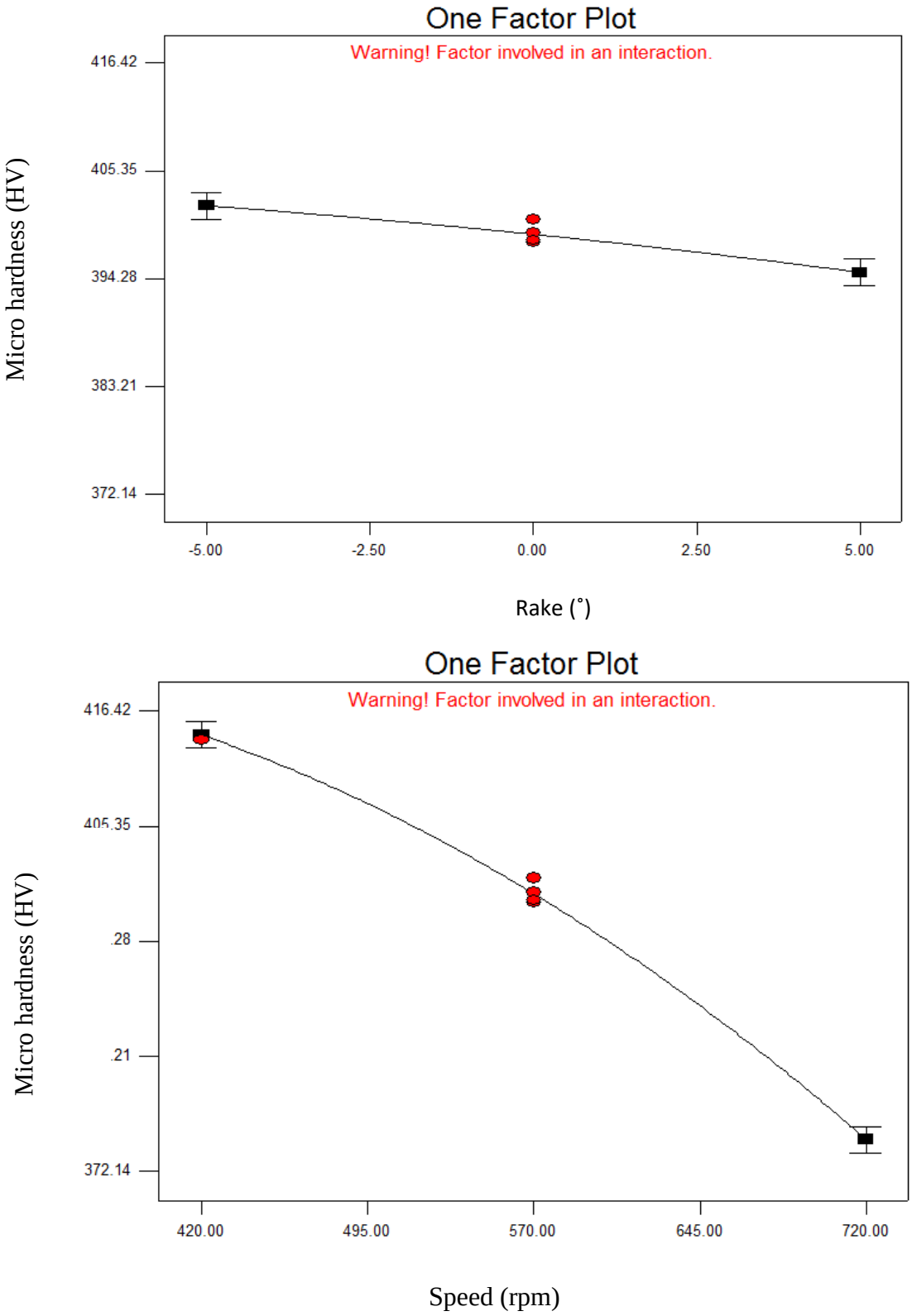

Figure5.3: Variation of (a) micro hardness v/s rake and (b) micro hardness v/s speed

For a given rake angle, as the cutting speed increases temperature in the PDZ increases which promotes grain growth in the material, because of which the hardness of the material

decreases. Dinakar Sagapuram et al. have studied the effect of cutting speed on hardness and deformation temperature and a similar trend was observed as in their study.

4.2.3 Analysis for surface roughness:

Mitutoyo model SJ-400 tester was used for measurement of surface roughness. The tester uses a stylus method of measurement. Tester has a profile resolution of 12nm and surface roughness can be measure upto 100µm. In this experiment tracing length of 4.8 mm was used.
The equation developed for response surface roughness is given below:

$$\text{Surface roughness} = 3.073 + 0.0228 \times A - 0.0021 \times B - 3.625 \times C - 0.05 \times A \times A + 0.0000007 \times B \times B + 17 \times C \times C - 0.0003 \times A \times B + 0.29 \times A \times C - 0.0017 \times B \times C$$

Table5.3: ANOVA table for surface roughness

SOURCE	SUM OF SQUARES	DF	MEAN SQUARE	F-VALUE	PROB>F	% contribution	STATUS
Model	6.89	9	0.77	87.09	<0.0001		Significant
A	0.049	1	0.049	5.61	0.0497	6.62	Significant
B	0.090	1	0.090	10.20	0.0152	1.21	Significant
C	0.010	1	0.010	1.14	0.3204	.13	Not Significant
A^2	6.58	1	6.58	747.91	<0.0001	88.99	Significant
B^2	0.0002632	1	0.0002632	0.002992	0.9579	.002	Not Significant
C^2	0.007605	1	0.007605	0.86	0.3834	.09	Not Significant
AB	0.034	1	0.034	3.89	0.0892	.473	Not Significant
AC	0.021	1	0.021	2.39	0.1660	.28	Not Significant
BC	0.0001	1	0.0001	0.011	0.9181	.001	Not Significant
Residual	0.062	7	0.008796				
Lack of fit	0.046	3	0.015	3.93	0.1096		Not Significant
Pure Error	0.16	4	0.0039			2.16	
Cor total	6.96	106					

Significant Factor: A, B, A^2

Insignificant factor*:* C,B^2, AB, AC, BC

In the following model we have taken interaction between A(rake), B(speed) , C (feed) , there squares A^2 , B^2 ,C^2 and also interaction between them AB , BC , CA.

Following things can be observed from analysis:

1. Model "F-Value" is 87.09 which imply model is significant. There is only 0.01% chance that model with this large value could occur due to noise.
2. Values of "Prob>F" lest than 0.05 indicates that model terms are significant. For given model A (Rake angle), B (Speed) and A^2 (square of rake angle) are significant.
3. Values greater than 0.1 are totally insignificant.
4. The "Lack of Fit-F value" of 3.93 implies that Lack of Fit is not significant relative to pure error.
5. As we can see A^2 factor has the maximum contribution in the model with % contribution of 88 % which implies it is the most important factor in the model.

There is 10.96% chance that "Lack of Fit-F value" this large could not occur due to noise. Non significant lack of fit is good .We want model to be fit.

The values of R-Squared given by software are as follows

Table 5.4: Diffrent ANOVA parameters

R- Squared	0.9911
Adj R-Squared	0.9798
Pred R-Squared	0.8908
Adeq Precision	22.260

- The "Pred R-Squared value" of 0.8908 is reasonable agreement with the "Adj R-Squared value" of 0.9798.
- "Adequate precision "value measure signal of noise ratio. It is desirable to have ratio greater than 4. Ratio of 22.260 indicates adequate signal. Hence model can be used.

The dependency of surface roughness on cutting speed and rake angle is shown in figure 5.4. Surface roughness of the samples decreases with increase in cutting speed and rake angle and with increase in feed surface roughness initially increases and then decreases. The reason being, with at low cutting speeds, matrix material is deformed to a lesser extent leading to discontinuous chip formation with cracks and higher surface roughness.With increasing rake angle, cutting forces and power consumption reduces

causing less heat generation and tool wear which further promotes continuous chip flow with reduced surface roughness.

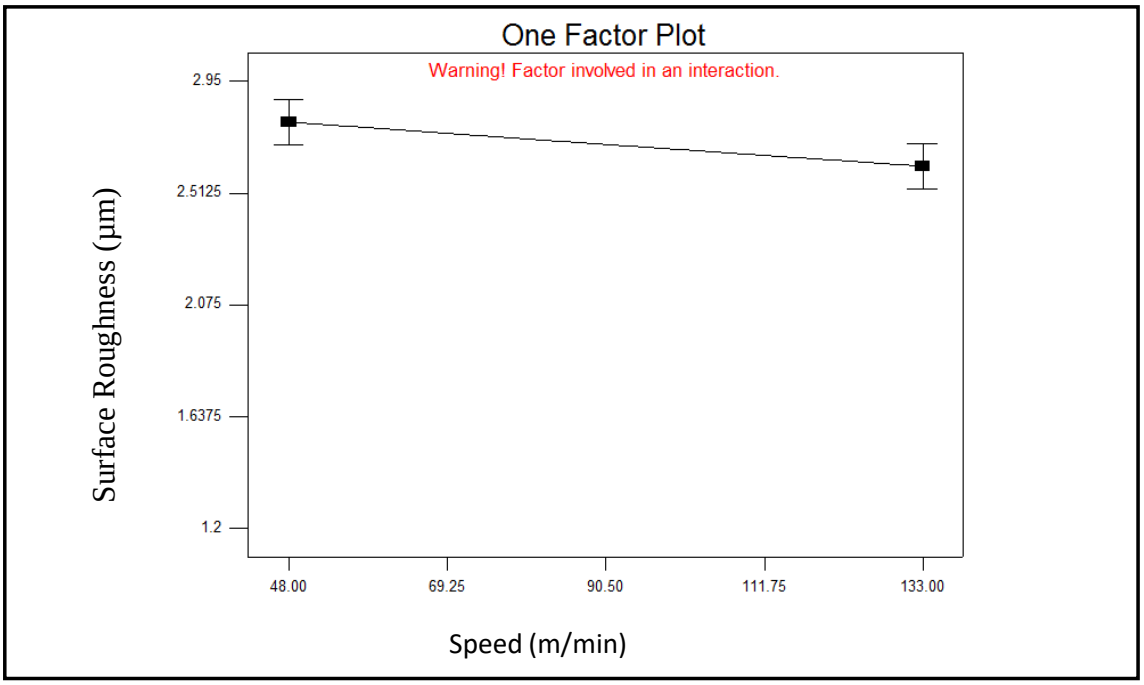

(a)

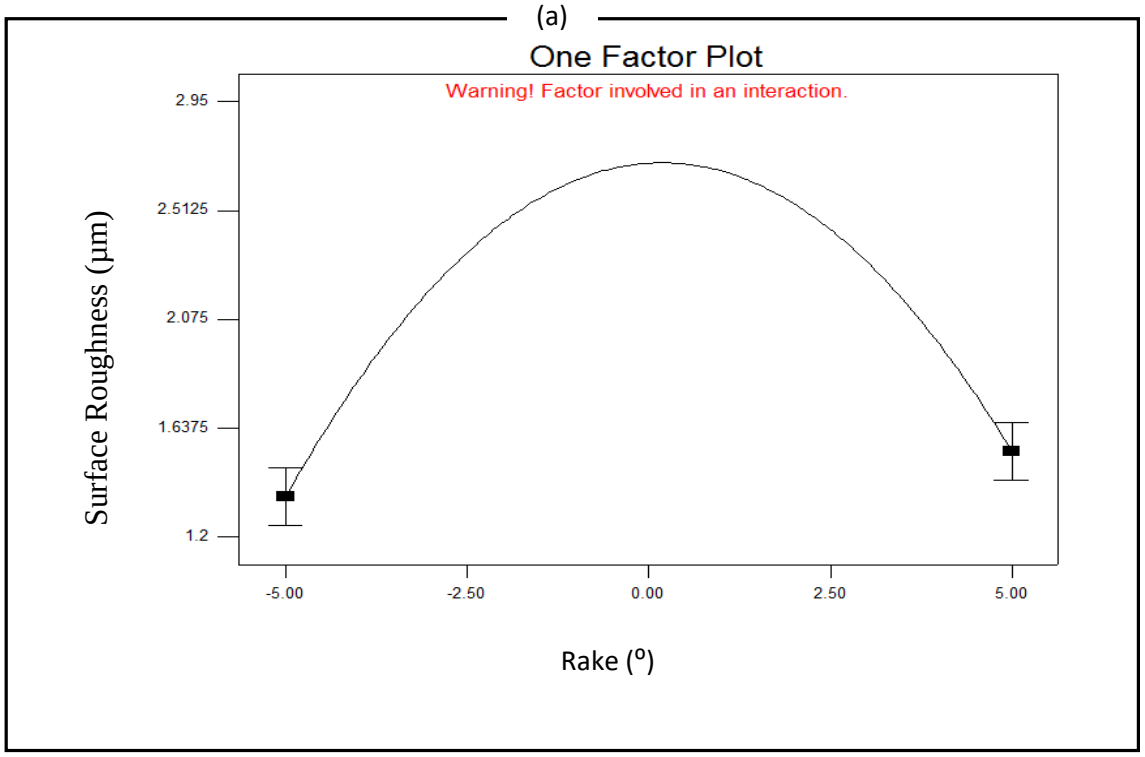

i.

Figure5.4: Variation of (a) surface roughness v/s speed and (b) surface roughness v/s rake

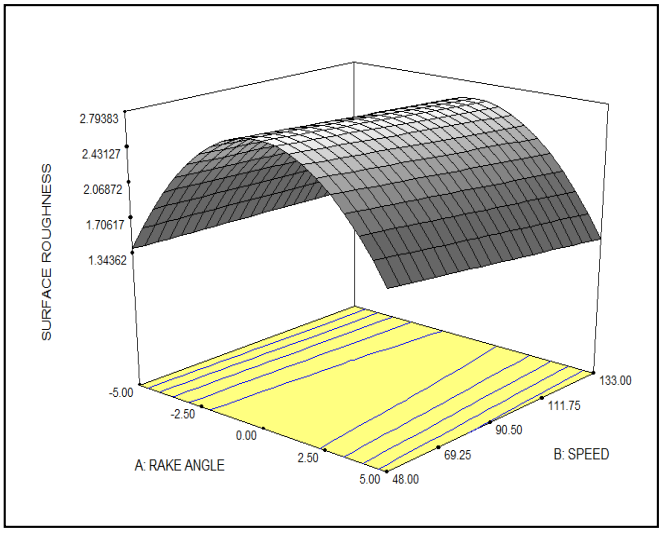

(a)

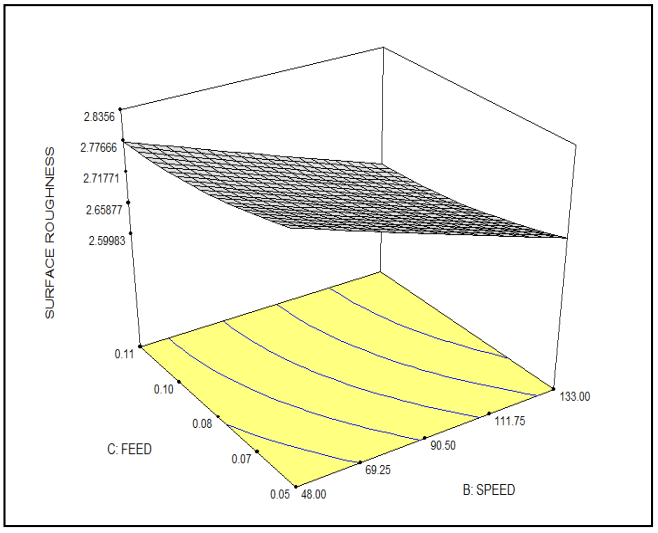

(b)

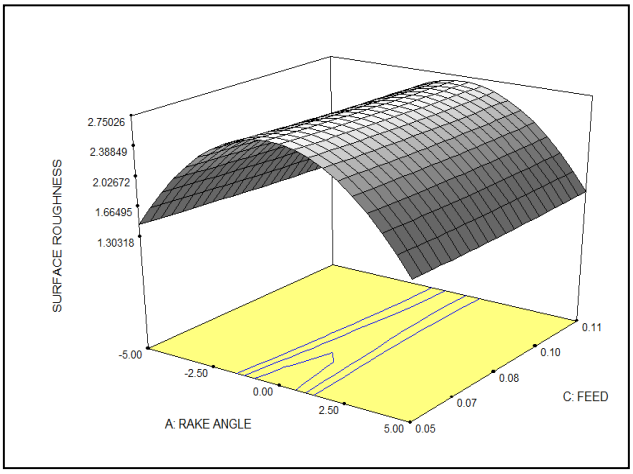

(c)

Figure5.5: 3-D plot of variation of (a) speed and rake v/s surface roughness (b) speed and feed v/s surface roughness (c) rake and feed v/s surface roughness

5.2.3 Result for shear strain:

In the Large strain extrusion Machining process severe plastic deformation is imposed on strips produced. In order to measure the level of deformation in strips, the shear deformation is carried out. Chip formation in machining occurs by concentrated shear in a narrow deformation zone, called the shear plane. In studies it was found that the shear strain increased with chip thickness ratio, it also increased with decrease in rake angle (α).

The mathematical relations of metal cutting process used to calculate chip thickness ratio (λ), shear strain (γ) and other parameters are described as follows. Chip thickness ratio (λ) can be expressed as

$$\lambda = \frac{t_c}{t}$$

Where t_c = deformed chip thickness and t= undeformed chip thickness

The shear strain can be expressed as

$$\gamma = \frac{\lambda}{\alpha} + \frac{1}{\lambda cos\alpha} - 2\tan\alpha$$

Where α denotes tool rake angle, λ is the chip thickness ratio of the chip and γ is the shear strain.

Effective strain (E_{eff}) may be expressed as:

$$E_{eff} = \frac{\gamma}{\sqrt{3}}$$

The value of undeformed chip thickness for all trails is 300 µm.

Table 5.5: The values of shear strain and effective strain at different deformation conditions

Rake(º)	Speed(m/min)	Chip compression ratio (λ)	Shear strain (γ)	Effective strain $E_{eff} = \frac{\gamma}{\sqrt{3}}$
0	720	1.33	2.08188	1.201974
0	720	1.36	2.095294	1.209719
5	570	1.16	1.854816	1.070878
5	720	1.18	1.860225	1.074001
-5	420	1.09	2.190077	1.264441
-5	720	1.11	2.19356	1.266452
5	570	1.15	1.852302	1.069427
0	570	1.42	2.124225	1.226422
-5	570	1.09	2.190077	1.264441
0	420	1.31	2.073359	1.197054

0	420	1.39	2.109424	1.217877
0	570	1.35	2.090741	1.20709
0	570	1.45	2.139655	1.23533
-5	570	1.12	2.195523	1.267586
0	570	1.39	2.109424	1.217877
0	420	1.40	2.114286	1.220683
5	420	1.21	1.869248	1.079211

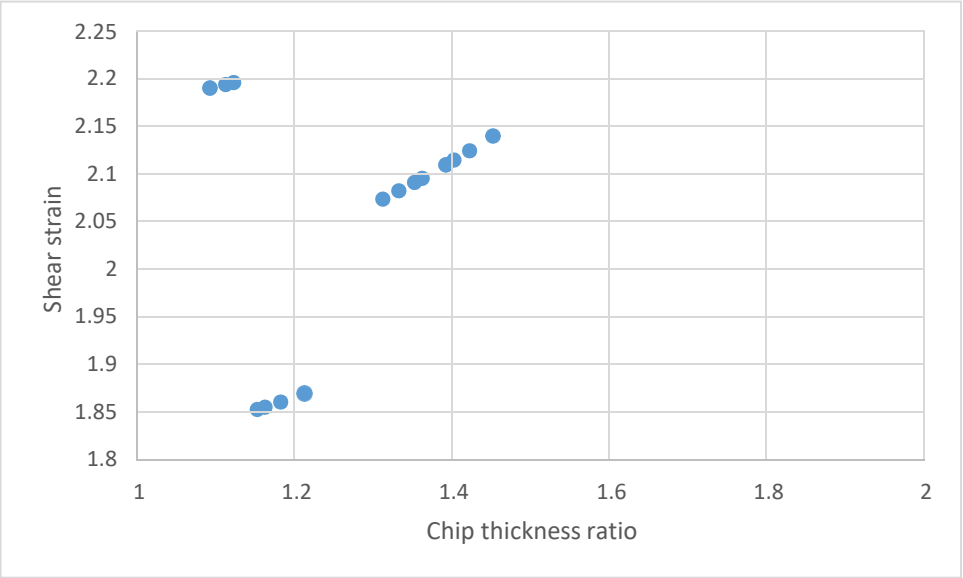

Figure 5.6: Variation of chip thickness ratio vs Shear strain

5.2.4 Result for XRD:

XRD analysis was done to study crystallographic deformation in the chips. Six peaks were taken from the result to analyze the sample.

Table 5.6: Crystallite size of Ti6Al4V samples investigated at different machining conditions from XRD

	Position 2θ(deg)	Height (counts)	FWHM 2θ(deg)	Area (counts*2θ)	Integral breadth(area/height) β_{exp}(degree)	Crystallite size (nm)
1.Bulk titanium						
1	38.8465	8540.84	0.2047	2586.58	0.302	95
2	42.0894	5349.99	0.0895	708.85	0.132	
3	63.3426	686.8	0.1404	192.85	0.280	
4	77.4192	1416.43	0.1872	530.31	0.374	
5	81.6825	700.85	0.0936	131.2	0.187	
6	93.2128	258.43	0.1872	96.76	0.374	
2.Titanium strips made at -5°rake and V=420 rev/min						
1	38.7912	4881.3	0.2558	1847.87	0.378	40
2	42.085	3562.85	0.1468	333.48	0.093	
3	63.3468	523.24	0.2303	178.27	0.340	
4	78.5202	1161.13	0.1092	253.59	0.218	
5	81.6191	439.57	0.307	199.68	0.454	
6	93.332	181.89	0.3744	136.2	0.748	
3.Titanium strips made at -5° rake and V=570rev/min						
1	38.8303	6876.34	0.1919	1952.33	0.283	49.1
2	42.9759	4417.05	0.2175	1421.3	0.321	
3	63.6135	484.26	0.1092	105.76	0.218	
4	77.484	1483.93	0.1716	509.28	0.343	
5	82.7288	459.41	0.1872	172	0.374	
6	93.308	222.27	0.2808	124.83	0.561	
4. Titanium strips made at -5°rake and V=720 rev/min						
1	38.8662	4267.96	0.1716	1464.76	0.343	52.2
2	42.1845	4050.8	0.2808	2274.93	0.561	
3	63.4482	626.63	0.1404	175.96	0.280	
4	77.5832	1307.12	0.1092	285.47	0.218	
5	82.7706	461.08	0.2184	201.4	0.436	
6	93.3543	233.23	0.2184	101.87	0.436	
5. Titanium strips made at 0°rake and V=420 rev/min						
1	38.7531	5979.52	0.2047	1810.88	0.302	63.8

2	43.0957	4226.74	0.2652	2241.86	0.530	
3	63.472	556.43	0.178	86.8	0.155	
4	77.5458	1447.12	0.1716	496.65	0.343	
5	82.7148	656.93	0.1092	143.47	0.218	
6	93.2743	228.91	0.1248	57.14	0.249	
6. Titanium strips made at 0° rake and V=570 rev/min						
1	38.8455	4778.37	0.1768	542.67	0.113	65.2
2	43.0333	4750.66	0.1404	1333.98	0.280	
3	63.4079	722.77	0.1716	248.06	0.343	
4	78.503	1500.09	0.156	468.03	0.312	
5	81.6967	366.14	0.1092	79.96	0.218	
6	93.2934	238.05	0.1936	44.56	0.187	
7. Titanium strips made at 0°rake and V=720 rev/min						
1	38.0356	3756.71	0.156	1172.09	0.311	68.4
2	42.3296	2919.97	0.1468	273.31	0.093	
3	63.605	472.69	0.178	73.74	0.156	
4	77.724	975.5	0.1404	273.92	0.280	
5	82.8795	292.37	0.1092	63.85	0.218	
6	93.4871	191.78	0.1872	71.8	0.374	
8. Titanium strips made at +5°rake and V=420rev/min						
1	38.8196	5929.27	0.2175	1907.9	0.321	71.8
2	43.1316	3249.41	0.156	1013.82	0.312	
3	63.4943	658.3	0.1092	143.77	0.218	
4	77.6089	1026.12	0.2496	512.24	0.499	
5	82.784	494.46	0.1092	107.99	0.218	
6	93.3545	149.61	0.1248	37.34	0.249	
9.Titanium strips made at +5°rake and V=570 rev/min						
1	38.8237	7898.06	0.1791	2092.92	0.264	75.2
2	43.9987	5028.23	0.2047	1522.79	0.302	
3	63.4241	764.16	0.1716	262.26	0.343	
4	77.4801	1351.44	0.1404	379.48	0.280	
5	82.7233	606.86	0.1404	170.4	0.280	
6	93.2764	244.37	0.0936	45.75	0.187	
10.Titanium strips made at +5°rake and V= 720rev/min						
1	38.8456	8540.84	0.2047	2586.58	0.302	82.32
2	43.0789	5349.99	0.0895	708.85	0.13	

3	63.4026	686.8	0.1404	192.85	0.280
4	77.5736	1416.43	0.1872	530.31	0.374
5	82.7526	700.85	0.0936	131.2	0.187
6	93.3526	258.43	0.1872	96.76	0.374

5.2.5 Result for SEM:

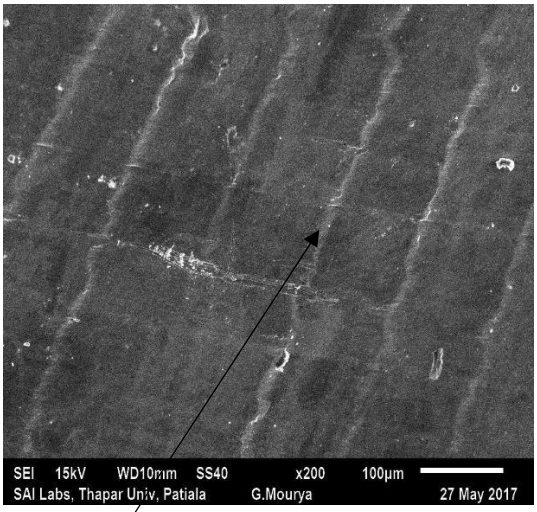

(a)

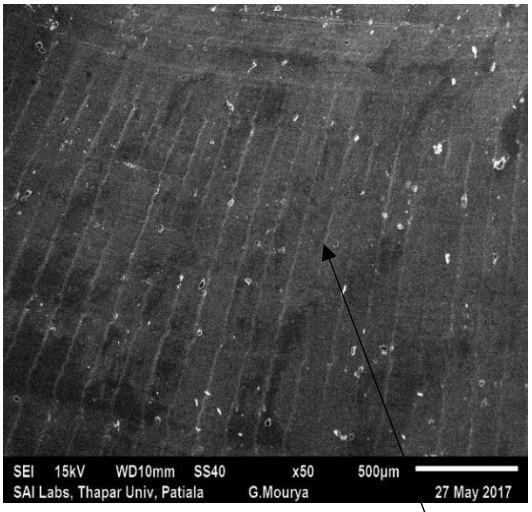

(b)

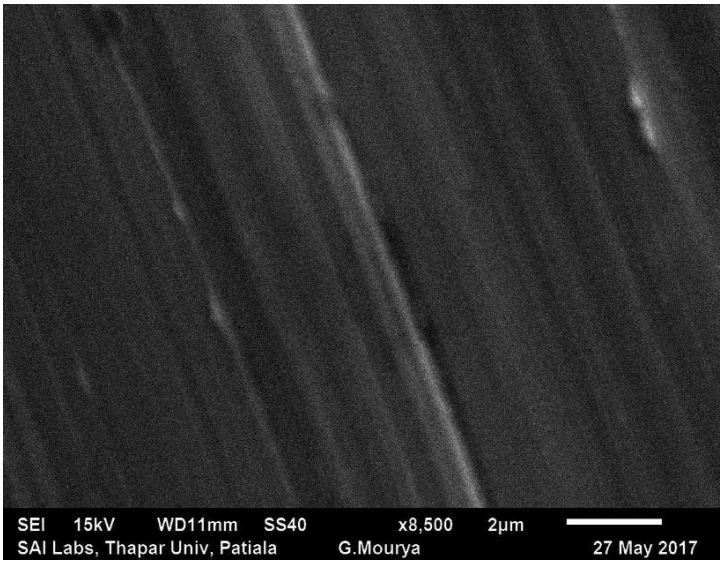

(c)

It is evident that there is formation of saw-tooth chip. If we compare the saw-tooth chip at different cutting speed then it is found that there is a transition of saw-tooth from aperiodic at low speed to periodic at high speed.

These saw-tooth occur within the primary shear zone due to thermo plastic instability. At low speed deformation in primary zone is due to cleavage and at high speed it is due to ductile facture.

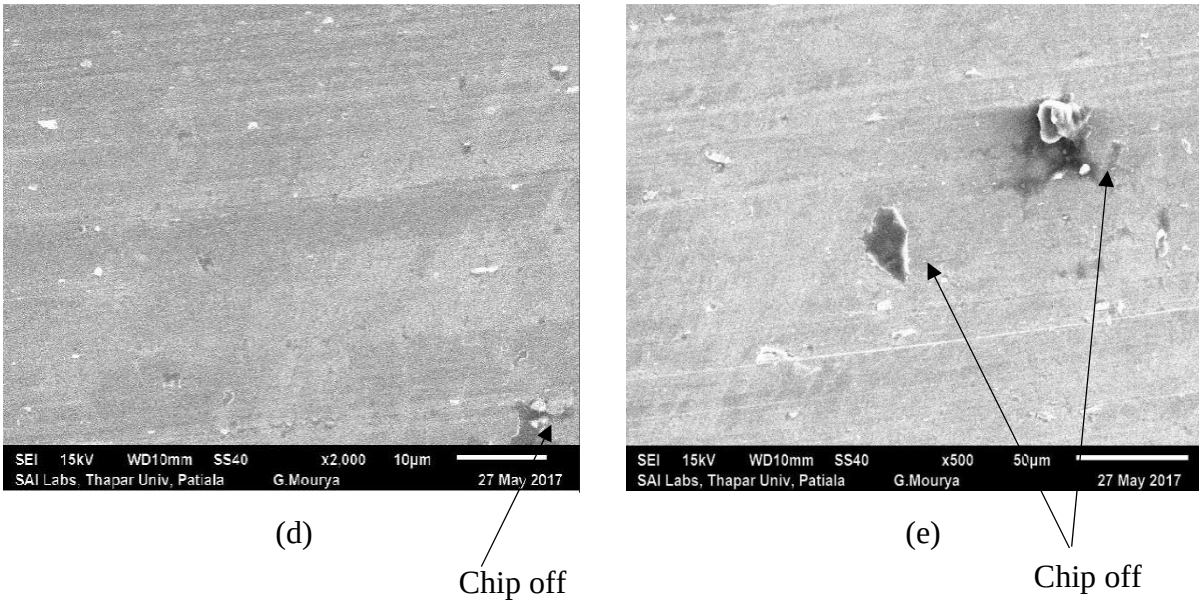

Figure 5.7: (a) SEM image of chip at 720 rpm (b) SEM image of chip at 570 rpm (c) SEM image of chip at 420 rpm (d) SEM image of chip at 720 rpm (e) SEM image of chip at 570 rpm

If we compare figure 5.7 (d) and figure 5.7 (d), chips are more prominent to chip off at high cutting speed. Chips those fabricated at 720 rpm chip off more in comparison to those fabricated at 570 rpm.

5.2.6 Result for micro hardness:

Table 5.7: Result for micro hardness for different trials

Rake(°)	Speed(m/min)	Feed(mm)	Micro hardness
0	720	0.05	374.49
0	720	0.15	374.93
5	570	0.05	393.13
5	720	0.10	372.14
-5	420	0.10	416.62
-5	720	0.10	377.66

5	570	0.15	394.87
0	570	0.10	397.98
-5	570	0.05	402.09
0	420	0.10	413.68
0	420	0.15	414.96
0	570	0.10	398.24
0	570	0.10	398.99
-5	570	0.15	401.88
0	570	0.10	400.37
0	420	0.05	413.12
5	420	0.10	410.71

5.2.7 Result for surface roughness:

Table 5.8: Result for surface roughness for different trails

Rake(^{o})	Speed(m/min)	Feed(mm)	Surface roughness
0	720	0.05	0.36
0	720	0.15	0.32
5	570	0.05	0.48
5	720	0.10	0.38
-5	420	0.10	0.42
-5	720	0.10	0.46
5	570	0.15	0.56
0	570	0.10	0.39
-5	570	0.05	0.63
0	420	0.10	0.38
0	420	0.15	0.31
0	570	0.10	0.37

0	570	0.10	0.40
-5	570	0.15	0.54
0	570	0.10	0.41
0	420	0.05	0.44
5	420	0.10	0.37

CHAPTER 6

CONCLUSION AND FUTURE SCOPE

6.1 Conclusion

On the basis of work conducted on Ti6Al4V titanium alloy chips, mechanical and microstructural properties were studied and following conclusions were drawn:

1. A valid model was obtained for responses such as surface roughness and micro hardness.
2. With increase in rake angle shear strain decreases and shear strain increases with increase in chip compression ratio.
3. Micro hardness of the fabricated chips was higher than that of ingot Ti6Al4V titanium alloy.
4. The increase in deformation level in chips is due to increase in strain resulting in decrease in crystalline size.
5. The crystalline size of fabricated chips is lesser than that of Ti alloy hence enhances the mechanical properties.
6. The formation of saw-tooth in primary deformation zone is due to thermo plastic instability.

6.2 Future scope of work:

1. A lot can be done to study the wear resistance properties of nanostructured material fabricated by LSM.
2. Shape of the chip formed by this process limits its usability in wide range since a better model can be prepared to have more control over its shape.

References

1. H. Gleiter. (2000) Nanostructured materials: basic concepts and microstructure. *Acta Mater*, 48: 1–29.
2. David D. Gill, Pin Yang, Aaron C. Hall, Tracy J. Vogler, Timothy J. Roemer, D. Anthony Fredenburg, Christopher J. Saldana. (2008) Creating Bulk Nanocrystalline Metal. SAND2008-6547: 1-92.
3. R.M. German. (1994) Source Powder Metallurgy Science. *Metal Powder Industries Federation*. ISBN 1-878954-42-3: 1-472.
4. S H Whang. (2011) Nanostructured metals and alloys. Woodhead Publishing. ISBN: 978-1-84569-6702: 1-840.
5. Nieman, G.W., J.R. Weertman, and R.W. Siegel. (1989) Microhardness of nanocrystalline palladium and copper produced by inert-gas condensation. *Scripta Metallurgica,*, 23: 2013-2018.
6. H. J. Fecht, E. Hellstern, Z. Fu, W. L. Johnson. (1990) 'Nanocrystalline metals prepared by high-energy ball milling. *Material Transcations A*, 21: 2333.
7. M. Ravi Shankar, Balkrishna C. Rao, Seongeyl Lee, Srinivasan Chandrasekar, Alexander H. King, W. Dale Compton. (2006) Severe plastic deformation (SPD) of titanium at near-ambient temperature. *Acta Materialia*, 54: 3691–3700.
8. M. Ravi Shankar, Srinivasan Chandrasekar, Alexander H. King, W. Dale Compton. (2005) Microstructure and stability of nanocrystalline aluminum 6061 created by large strain machining. *Acta Materialia*, 53: 4781–4793.
9. J. K. Jim, H. G. Jeong, S. I. Hong, Y. S. Kim and W. J. Kim.
10. S. Shekhar, S. Abolghasem, S. Basu, J. Cai and M. R. Shankar. (2012) Effect of Severe Plastic Deformation in Machining Elucidated via Rate-Strain-Microstructure Mappings. *Journal of Manufacturing Science and Engineering*. 134: 031008-1.
11. S. Shekhar, S. Abolghashem, S. Basu, J. Cai, and M. Ravi Shankar. (2012) Interactive Effects of Strain, Strain-Rate and Temperatures on Microstructure Evolution in High Rate Severe Plastic Deformation. *Materials Science Forum*. 702-703: 139-142.
12. C. Huang, T.G. Murthy, M.R. Shankar, R. MSaoubi and S. Chandrasekar. (2008) Temperature rise in severe plastic deformation of titanium at small strain-rates. *Scripta Materialia,* 58: 663–666.

13. S. Swaminathan, T.L. Brown, S. Chandrasekar, T.R. McNelley, and W.D. Compton. (2007) Severe plastic deformation of copper by machining: Microstructure refinement and nanostructure evolution with strain. *Scripta Materialia* ,56: 1047–1050.
14. R. Calistes, S. Swaminathan, T.G. Murthy, C. Huang, C. Saldana, M.R. Shankar and S. Chandrasekar. (2009) Controlling gradation of surface strains and nanostructuring by large-strain machining. *Scripta Materialia* ,60: 17–20.
15. Andrew Kustas, Kevin Chaput, Srinivasan Chandrasekar, Kevin Trumble. (2014) Quality of strips produced by extrusion machining directly from Cast 5052 Aluminum. *Material science and technology,* 2014: 79-86.
16. W.J. Deng ,Q. Li ,B. Li, Z.C. Xie , Y.T He ,Y Tang and W. Xia. (2014) Thermal stability of ultrafine grained aluminium alloy prepared by large strain extrusion machining. *Materials Science and Technology* , 30,(7): 850-859.
17. Dinakar Sagapuram, Andrew B. Kustas, W. Dale Compton, Kevin P. Tumble, Srinivasan Chandrasekar. (2015) Direct Single-Stage Processing of light weight alloys into sheet by hybrid cutting extrusion. *Journal of Manufacturing Science and Engineering,* 137: 1-10.
18. Travis L. Brown, Christopher Saldana, Tejas G. Murthy, James B. Mann, Yang Guo, Larry F. Allard, Alexander H. King, W. Dale Compton, Kevin P. Trumble, Srinivasan Chandrasekar. (2009) A study of the interactive effects of strain, strain rate and temperature in severe plastic deformation of copper. *Acta Materialia,* 57: 5491–5500.
19. S. Chandrasekhar ,K.P Trumble,W. Moscoso,Mert Efe , D. Sangapuram ,CJ. Saldana,J.B. Mann ,W.D Crompton. (2014) Large strain extrusion machining processes and bulk produces therefrom. US Patent: 0017113.
20. M. Ravi Shankar, Srinivasan Chandrasekar, W. Dale Compton, Alexander H. King. (2005) Characteristics of aluminum 6061-T6 deformed to large plastic strains by machining. *Materials Science and Engineering*, 410–411: 364–368.
21. Srinivasan Swaminathan, M. Ravi Shankar, Seongyl Lee, Jihong Hwang, Alexander H. King, Renae F. Kezar, Balkrishna C. Rao, Travis L. Brown, Srinivasan Chandrasekar, W. Dale Compton, Kevin P. Trumble. (2005) Large strain deformation and ultra-fine grained materials by machining. Materials Science and Engineering, 410–411: 358–363.
22. J.B. Mann, C. Saldana, S. Chandrasekar, W.D. Compton and K.P. Trumble. (2007) Metal particulate production by modulation-assisted machining. *Scripta Materialia*, 57: 909–912.

23. Andrew Kustas, Kevin Chaput, Srinivasan Chandrasekar, Kevin Trumble. (2014) Quality of strips produced by extrusion machining directly from Cast 5052 Aluminum. *Material science and technology,* 79-86.
24. Mert Efe, Wilfredo Moscoso, Kevin P. Trumble, W. Dale Compton, Srinivasan Chandrasekar. (2012) Mechanics of large strain extrusion machining and application to deformation processing of magnesium alloys. *Acta Materialia,* 60: 2031–2042
25. Seongeyl Lee, Jihong Hwang, M. Ravi Shankar, Srinivasan Chandrasekar, and W. Dale Compton. (2005) Large Strain Deformation Field in Machining. Metallurgical and materials transactions, 37A: 1633.
26. P. Iglesias, M. D. Bermudez, W. Moscoso and S. Chandrasekar. (2010) Influence of processing parameters on wear resistance of nanostructured OFHC copper manufactured by large strain extrusion machining, *Wear* 268: 178–184.
27. P. Iglesias, W. Moscoso, J.B. Mann, C. Saldana, M. R. Shankar, S. Chandrasekar, W. D. Compton and K. P. Trumble. (2008) Production analysis of new machining-based deformation processes for nanostructured materials. *International Journal of material forming,* 1:459–462.